



Application of transition state theory to the study of materials containing acryloxy and acrylate units

Vassilios Galiatsatos*, B. Jeffrey Sherman

Institute of Polymer Research-Dresden, Hohe Strasse 6, D-01069 Dresden, Germany

Available online 13 April 2005

Dedicated to Professor J.E. Mark on the occasion of his 70th birthday.

Abstract

We study the diffusion behavior of a probe, in monomers containing acryloxy and acrylate units that are commonly used in restorative dentistry. We apply a version of transition state theory with satisfactory results. Results show that transition state theory describes part of the underlying physics successfully thus reinforcing its applicability as a complement and extension to molecular dynamics simulations. © 2005 Elsevier Ltd. All rights reserved.

Keywords: Modeling; Transition state theory; Dental polymeric materials

1. Introduction

We study the diffusion of a helium probe in systems consisting of 2,2-bis[4-(2-methacryloxypropoxy)phenylene]propane (Bis-GMA), ethoxylated bisphenol-A dimethacrylate (EBPADM) and a mixture of Bis-GMA and triethylene glycol dimethacrylate (TEGDMA) (70%/30%) (Fig. 1).

Bis-GMA is one of the most commonly used polymeric dental restorative materials. It is part of several polymeric composite resins currently used for tooth restoration. Bis-GMA by itself is far too viscous to be used directly. The reason it is so viscous is that the side chains with the polar hydroxy groups are separated by a relatively inflexible central ring system. This configuration does not allow the rotation of the –OH groups to lower energy intramolecular hydrogen bonded configurations and thus, intermolecular hydrogen bonding occurs [1,2]. To decrease this intermolecular hydrogen bonding, and lower the viscosity, a composite resin normally consists of two dimethacrylate monomers, Bis-GMA and a lower molecular weight diluent, generally tri-ethylene glycol dimethacrylate (TEGDMA). In

fact a 60/40 mix of Bis-GMA/TEGDMA is 50 times less viscous than Bis-GMA alone. In addition to the monomers, filler is added to the resin (between 45 and 85 mass%) to produce a stronger, more wear resistant system that has lower polymerization volume shrinkage and lower thermal expansion [3]. It is also quite beneficial to rely on finite element methods (FEM) for the structural optimization of the filling's geometry.

The main drawback of the polymeric composite resins is their overall lack of durability. The typical lifespan for posterior composite resins is between 3 and 10 years, normally less than five for large fillings [4]. The main cause for this lack of durability is internally induced stresses in the material [5]. These stresses can be caused by interactions with food, differences in thermal expansion, and volume shrinkage during polymerization.

The volume shrinkage during polymerization is the driving force for this study. Shrinkage during polymerization can be devastating to the healthy tooth structure as it can negatively affect the tooth by either adhesive or cohesive failure [6,7]. If the shrinkage causes adhesive failure (the restorative pulling away from the tooth) microcracks can form between the restoration and the tooth itself. These microcracks then allow bacteria to leak back into the tooth causing additional damage to the tooth. In addition, cohesive failure (the restorative or the tooth failing, while the adhesive layer stays intact) can occur. When cohesive failure occurs, a crack will either form in the center of the restorative again allowing intrusion of bacteria,

* Corresponding author. Address: Equistar Chemicals, 11530 Northlake Drive, Cincinnati, OH 45249, USA. Tel.: +1 513 530 4263.

E-mail address: vassilios.galiatsatos@equistarchem.com (V. Galiatsatos).

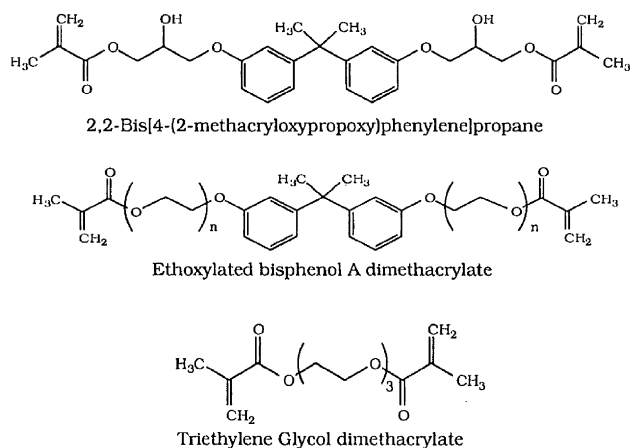


Fig. 1. Chemical structure from top to bottom of Bis-GMA, EBPADM and TEGDMA.

or the tooth could just shatter. In either case, the importance of limiting polymerization shrinkage cannot be overstated.

As a first step we aim to understand the free volume and diffusion characteristics of the components that go into these dental restoratives. One approach for evaluating diffusion coefficients D using molecular dynamics involves monitoring the mean-squared displacement $\langle r^2 \rangle$ of the diffusing species as a function of time. More precisely stated, the Einstein relation $D = \lim_{t \rightarrow \infty} \langle (r_t - r_0)^2 \rangle / 6t$, holds in the diffusive regime. Here \mathbf{r}_t is the position of the diffusing particle at time t and the angle brackets denote an average over an ensemble of systems. If the slope of a plot of $\langle r^2 \rangle = \langle (\mathbf{r}_t - \mathbf{r}_0)^2 \rangle$ with time is constant, the Einstein formula gives the diffusion coefficient of interest. The process of penetrant diffusion in rubbery and glassy polymers can be studied using the transition state theory, as formulated by Suter and co-workers [8–10] and as reviewed by Gusev et al. [11].

2. Computational procedure

According to transition state theory, the evolution of the polymer penetrant system in time is viewed as a Poisson process consisting of successive, uncorrelated jumps between neighboring macrostates [12]. Each jump of a probe from macrostate i to macrostate j is associated with a first-order rate constant k_{ij} .

Consider an ensemble of penetrant/polymer system with a distribution of probes throughout the macrostates at $t=0$; as time elapses, the distribution evolves through transitions between macrostates. Let $p(t)$ be the probability of finding a probe in macrostate i at time t . Now the quantity $p(t)$ evolves according to the equation:

$$\frac{dp_i}{dt} = - \sum_j k_{ij} p_i + \sum_j k_{ji} p_j \quad (1)$$

At very long times, the ensemble reaches its equilibrium distribution, so then the probability of finding a probe in the

macrostate i is p_i^{eq} . The equilibrium probabilities obey the condition of microscopic reversibility [13]:

$$k_{ij} p_i^{\text{eq}} = k_{ji} p_j^{\text{eq}} \equiv k_{ij} \quad (2)$$

Considering Eq. (1) and the normalization condition

$$\sum_i p_i^{\text{eq}} = 1 \quad (3)$$

the average residence time in macrostate i at equilibrium is:

$$\tau = \frac{1}{\sum_j k_{ij}} \quad (4)$$

Now with the rate constants and the residence time in each macrostate, the diffusion of the probe may be calculated.

In this work it is assumed that the penetrant motion is coupled with the thermal or vibrational motion of the polymer atoms (but not with structural relaxations of the polymer). The thermal motion of the polymer matrix is accounted for by using a ‘smearing parameter’ which is calculated based on displacements of the host atoms evaluated from a MD simulation.

Additionally using the full atomistic representation of the probe and the system under investigation, the computational intensiveness is too great to derive exact results [14]. Following Gusev and Suter, we employ several additional approximations in order to obtain reasonable computing times. In this revised transition state methodology, the approximations make certain calculations less intensive. For example, a spherical representation of the probe based on its diameter rather than its atomistic detail simplifies the evaluation of the rate constant.

In addition, there is no distinction between the states and macrostates. By using the latter approximation a large number of local minima are obtained. The system is then divided up into states and dividing surfaces by constructing a regular grid through the polymer configurations. The configurational integrals needed for the evaluation of p_i^{eq} and k_{ij} are then obtained through direct numerical integration over the values of the potential energy at the node points of the grid. The results of the analysis are then used to calculate the residence times of the penetrants in the states.

Now that the rate constants and residence times are obtained, a Monte Carlo jump process can be performed on the system. A probe molecule is ‘dropped’ into a system at a randomly chosen state. The initial state is typically selected with a probability that is proportional to the state’s residence time. Since each state has already been designated a residence time, the residence time of the probe in the specific state is added to the previous summation of the time of the simulation. For the initial step, the residence time will be added to $t=0$. Based now on the rate constant of the probe to jump to an adjacent state, the probe is moved a designated distance from the center of the previous state to the center of the next adjacent state. Again the residence time for that state is added to the previously accumulated

simulation time. This process continues until the accumulated time reaches a predetermined maximum. At this point, the probe has moved a specified distance from the original site over a given duration. This distance squared and then divided by the time results in the diffusion coefficient of the probe through the system. For each resin system, this Monte Carlo process is performed at least 500 times to confirm consistent diffusion coefficient results.

The modeling software used consisted of MSI/Accelrys Insight version 2.3.7, Discover version 2.9.5 and Amorphous Cell version 7.0. All simulations were performed at 308 K. Using one or more of the molecules as inputs, the amorphous cell is built. In addition to the molecules of interest, the mass density of the system, as well as the number of atoms to be used in the amorphous cell are used as input. Using the experimental density of the materials and choosing a number of atoms that insures no interchain interaction, around 2400 atoms (30–37 molecules), the average amorphous cell size is between 28 and 29 Å per side. Three to five different configurations of each cell are created as an attempt to confirm reproducibility.

The refinement is then performed on the built amorphous cell. An initial minimization of 200 steps is used to eliminate any unrealistic bond lengths or angles. A molecular dynamics run of 60,000 steps, 60 ps, is then performed. Mass densities for the systems were 1.133 g/cm³ for the Bis-GMA system and 1.100 g/cm³ for both the EBPADM and the Bis-GMA/TEGDMA mixed systems. The duration of this dynamics run affords standard deviations of the total energy of the system between 2 and 5% for each of the configurations. A final 1500 step minimization is then performed on the system, again to ensure all bond lengths and angles are correct.

To validate the system, a cohesive energy density calculation is performed on the cells. Cohesive energy, $-U$, is defined as the increase in energy per mole of a material if all intermolecular interactions are eliminated. Therefore, it is found by subtracting the sum of the total energy of the system and a tail correction, to ensure there has been no truncation effect on the energy, from the intramolecular energy of the parent molecules. The cohesive energy density, c , would then be the cohesive energy per unit volume, so that $c = -U/V$. This cohesive energy density value is compared to cohesive energy density values found using the respective molecules and applying graph-based QSPR theory [15]. The cohesive energy density found using this method is based on a large number of 76 experimental values, therefore, the cohesive energy density value is based on experimental work on similar or identical systems. Since, all of the properties used in this work are averaged over the number of configurations, the average of the cohesive energy density over the given number of configurations is studied. The system is considered valid if the cohesive energy densities from the two methods agree within 10%.

After the cell is constructed, refined, and validated

another molecular dynamics run is performed. This time a constant pressure dynamics run is performed with the value used for the pressure taken from the constant volume dynamics run, careful to confirm that the density of the system does not change after the constant pressure run has completed. With the constant pressure run complete, the free volume can be studied using the outlined transition state theory approach to follow the diffusion of a probe. At this point, all of the inputs are entered to follow the diffusion of the probe in the simulated dental resin system.

The first input is the type of probe. Helium was chosen. Next, the cell grid step, the distance between the grid points previously described, is chosen. For all work reported here a cell grid step of 0.5 Å is used. This grid step size was chosen based on computational considerations. The temperature and cutoff distances are also chosen, the temperature being the temperature of the experimental methods and the cutoff distance being 8.0 Å, a reasonable number with respect to the 0.5 Å grid step size.

The final input parameter that needs to be considered is that of the smearing factor value (between 0 and 1 Å). The smearing factor allows for the facilitation of the diffusion of the probe through the system. It ‘allows’ for elastic motions of the matrix that open and close the pathways between regions. The smearing factor was calculated from short-scale MD trajectories of the system in the absence of the probe. This method does require an initial guess of the smearing factor and then an optimization can be completed after a small number of calculations.

This free volume process now creates a data file with the number and size of the states within the cell. The next step is to obtain the diffusion coefficient. We utilize the output data file of the state information to create the trajectory. The only inputs are the data file, the number of times the jump process is to be performed (500 times for all systems), and the duration of each jump process. The distance the probe moves and the time needed to go the distance are both used to calculate the diffusion coefficient. If the gradient of $\log(\text{MSD})$ versus $\log(\text{time})$ was not unity over the last decade checked then the simulation time was increased in order to ensure true diffusion.

3. Results and discussion

An example of residence time results for one conformation of a system of Bis-GMA/TEGDMA is given in Fig. 2, where the probability of finding a state with the designated residence time is plotted versus the log of the residence time. One observes that the majority of sites is associated with a mean residence times around 10^{-12} s.

The state volume distribution data for one conformation of the system of Bis-GMA/TEGDMA is given in the chart of Fig. 3. The horizontal axis represents the log of the state volume, with volume in units of Å³ and the vertical axis

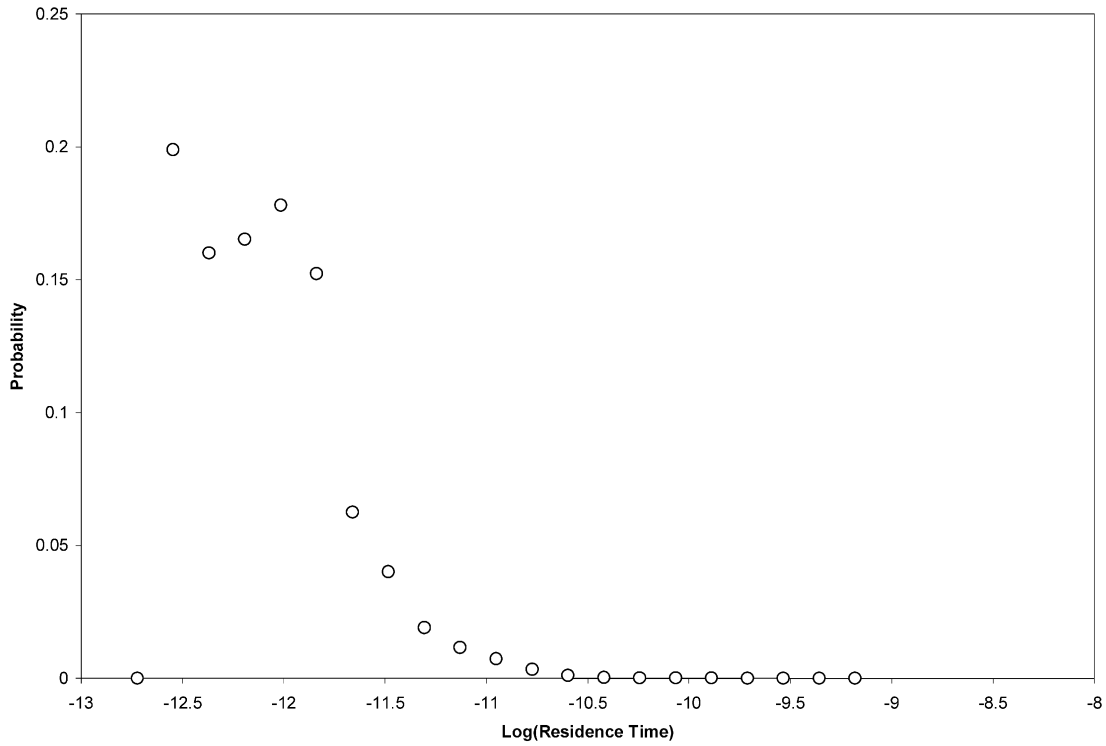


Fig. 2. The log of the residence time (in seconds) and the probability of finding that residence time for one conformation of a system of Bis-GMA/TEGDMA.

gives the number of sites with the corresponding log volume.

Typical plots with results from multiple conformations as well as the average plot are shown in Fig. 4.

The average of the diffusion coefficients of each of the configurations is used to give the ultimate diffusion coefficient for each system. The volume found for each state listed is then used when calculating the distance

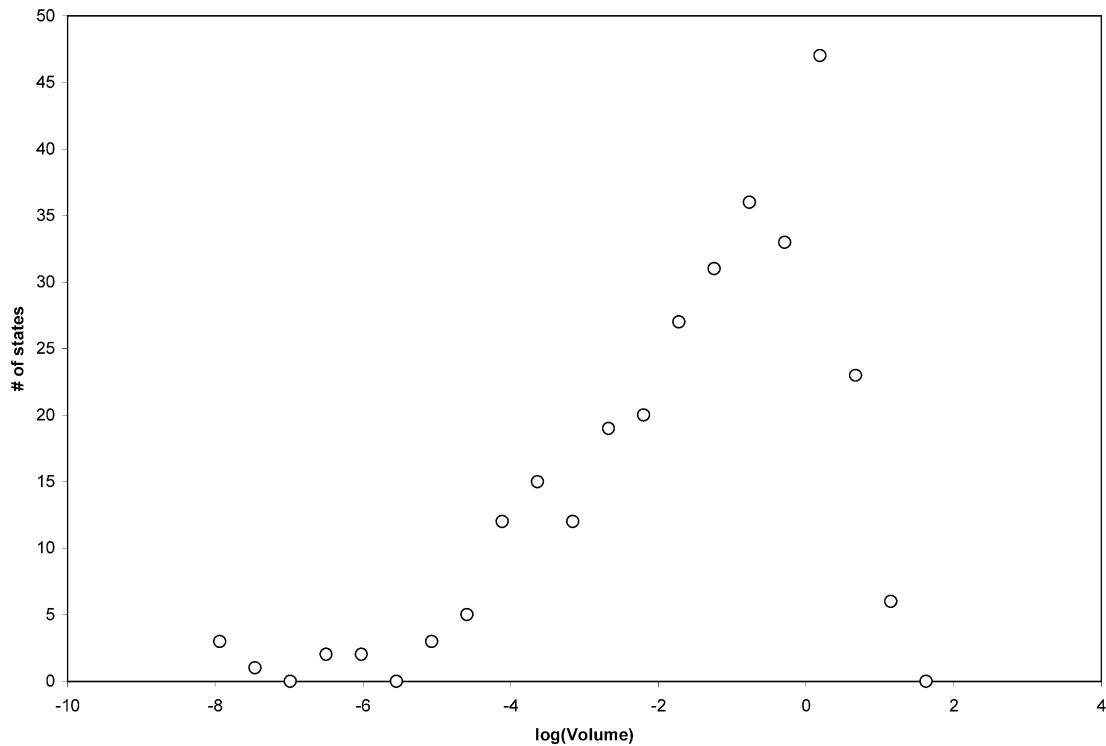


Fig. 3. The log of the volume of the states and the number of states with that volume for one conformation of a system of Bis-GMA/TEGDMA.

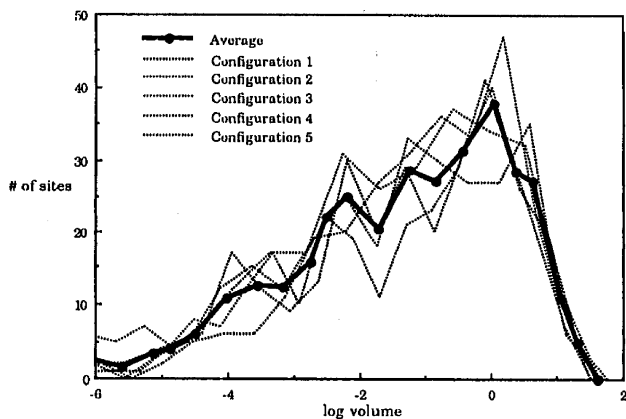


Fig. 4. State volume distribution for a conformation of a Bis/GMA/TEGDMA system.

between centers of states, which is ultimately used in the calculation of the length of the jump a probe makes from one state to the next. The culmination of all of these jumps is then given as a table of mean squared displacement versus time.

A plot of the mean square displacement versus time, Fig. 5, confirms that the diffusion coefficient found at the end of the diffusion simulation is in the true diffusion region and that the diffusion found is valid.

In the diffusion simulations, 500 attempts for moving the He molecule, each starting at an arbitrary state, were performed. Fig. 5 shows the time dependence of the mean squared displacement of the He atom dissolved in the computed system. Three different regions of probe mobility

are observed. The first one is limited by the distribution of the residence times at the initial sites and is terminated at around 10^{-11} s. The second region from 10^{-11} s up to approximately, 10^{-10} s reflects the microscopic packing inhomogeneity of the system. The distinct feature of this region is that the mean square displacement of the probe goes as t^n , with $n < 1$. This is probably a result of the free volume channels formed in the spatial web. Those are of rather complicated geometry and their dimensions are less than three.

The third regime, that of true diffusion ranges from approximately, 10^{-9} s and above. The straight line is drawn with a slope of unity and following the Einstein relationship described earlier one may calculate the diffusion coefficient of the probe in the system.

Table 1 shows the values of D for the three systems studied. One observes that for the EBPADM and Bis-GMA/TEGDMA systems the probe diffuses at a rather typical rate which is in the order of 10^{-6} s. This is in excellent agreement with published results of He diffusion in other glassy polymers [16].

The diffusion coefficient of the Bis-GMA system suggests that the probe moves an order of magnitude slower than in the other systems. This behavior merits further investigation. Explicit incorporation of polymer degrees of freedom during the calculation may lead to much lower, and more realistic, energy barriers for the transition state than those found in the current work. The influence of the size of the representative volume element should also be investigated further. One cannot obtain an efficient packing of

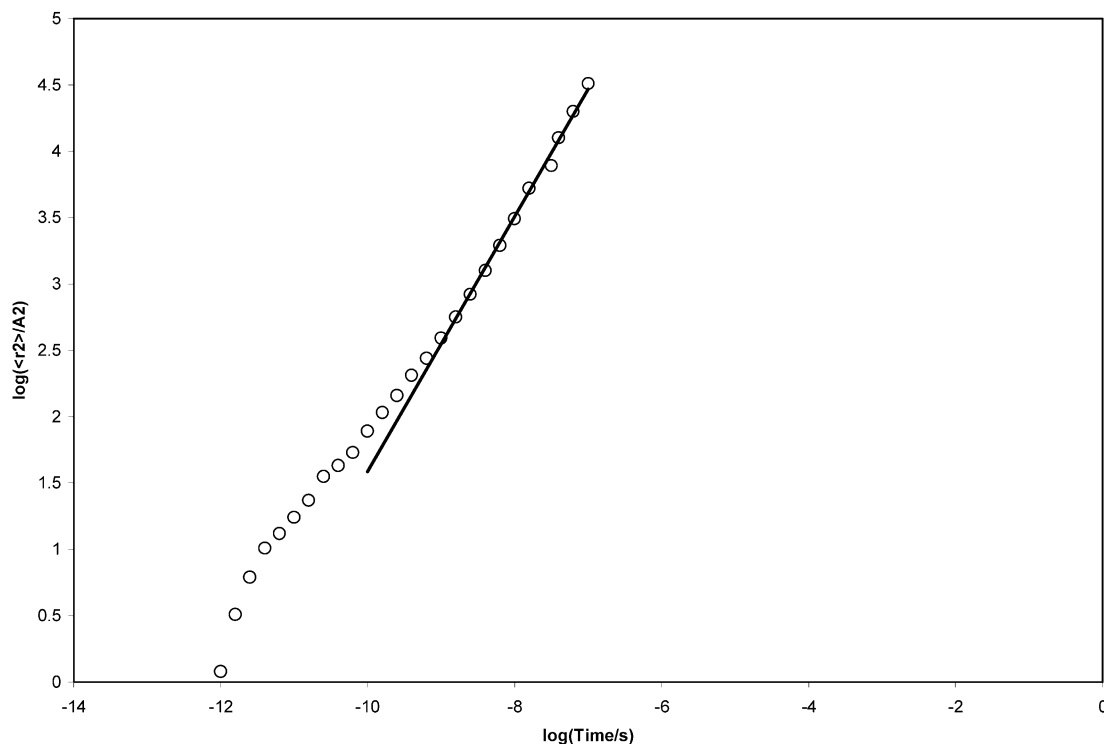


Fig. 5. Time dependence of the mean squared displacement of the He atom dissolved in the computed Bis-GMA/TEGDMA system.

Table 1
Log D values (units of cm^2/s) in each of the three resin systems

Resin system	Log D
Bis-GMA	−6.30
Ethoxylated bisphenol A dimethacrylate	−5.36
Bis-GMA/TEGDMA system	−5.58

molecules if the employed computer model is not large enough.

4. Conclusions

Diffusion of a helium probe gives results of the order of $10^{-6} \text{ cm}^2/\text{s}$ in good agreement with previous experience with glassy systems. This gives us confidence to further apply transition state theory to investigate free volume changes as crosslinking occurs. The Bis-GMA system yields values that are an order of magnitude lower than expected. At this point we reserve judgment as to the reasons behind this behavior. We speculate that modifications to the simulation method to take into account strong hydrogen bonding may yield more traditional values.

Acknowledgements

VG would like to express his gratitude to the Institute of

Polymer Research-Dresden and especially to Professor Dr Gert Heinrich for their hospitality and support during the summer of 2004 when part of this work was done.

References

- [1] Davy KWM. *J Mater Sci-Mater Med* 1994;5:350–5.
- [2] Sankarapandian M, Xu Q, McGrath JE, Taylor DF, Kalachandra SJ. *Adv Mater* 1996;28:59–67.
- [3] Anseth KS, Newman SM, Bowman CN. *Adv Polym Sci* 1995;122:177–201.
- [4] Bowen RL, Marjenhoff WA. *Adv Dent Res* 1992;6:44–51.
- [5] Kusy RP, Leinfelder KE. *J Dent Res* 1977;56:544–52.
- [6] Watts DC. *Mater Sci Technol* 1992;14:209–19.
- [7] Davidson CL. In: Vanherle G, Smith DC, editors. *Posterior composite resin dental restorative materials*. Amsterdam: Peter Szulc; 1985.
- [8] Gusev AA, Suter UW. *Phys Rev A* 1991;43(12):6488–94.
- [9] Gusev AA, Suter UW. *J Chem Phys* 1993;99(3):2221–7.
- [10] Gusev AA, Suter UW. *J Chem Phys* 1993;99(3):2228–34.
- [11] Gusev AA, Muller-Plathe F, van Gunsteren WF, Suter UW. *Adv Polym Sci* 1994;116:207–47.
- [12] Feller W. *An introduction to probability theory and its applications*. vol. II. New York: Wiley; 1957.
- [13] Theodorou D. In: Neogi P, editor. *Diffusion in polymers*. New York: Marcel Dekker; 1996.
- [14] Jagodic F, Borstnik B, Azman A. *Macromol Chem* 1973;173:221–4.
- [15] Bicerano J. *Prediction of polymer properties*. New York: Marcel Dekker; 1993.
- [16] Muruganandam N, Koros WJ, Paul DR. *J Polym Sci, Polym Phys Ed* 1987;25:1999–2013.